CrossMark

ORIGINAL PAPER: FUNCTIONAL COATINGS, THIN FILMS AND MEMBRANES (INCLUDING DEPOSITION TECHNIQUES)
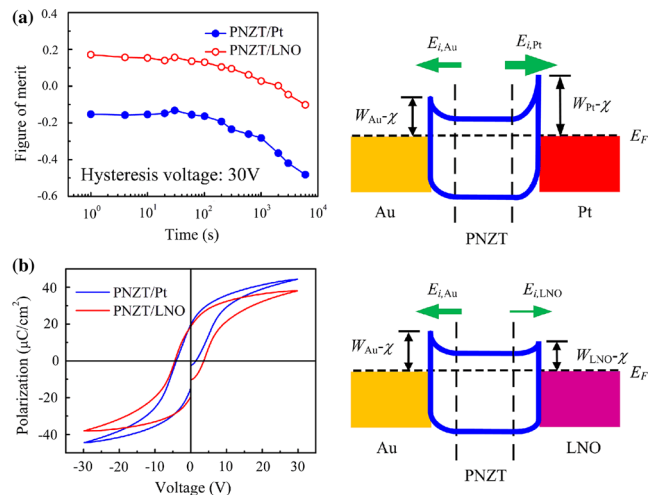
Effects of electrodes on ferroelectric properties of PNZT films prepared by sol–gel method

Quanliang Zhao[1] · Peipei Tan[1] · Guangping He[1] · Jiejian Di[1] · Dawei Wang[1] · Lihui Qi[1] · Haibo Jin[2] · Maosheng Cao[2]

Abstract Nb-doped lead zirconate titanate (PNZT) perovskite films have been prepared on $LaNiO_3/SiO_2/Si$ and $Pt/Ti/SiO_2/Si$ substrates using a sol–gel route. With the same Au top electrodes, the as-fabricated $PNZT/LaNiO_3$ film exhibits better ferroelectric fatigue property than that of PNZT/Pt film. The results of ferroelectric imprint show that the net internal electric fields toward the top and bottom electrodes can be built in $PNZT/LaNiO_3$ and PNZT/Pt films, respectively. Imprint failure of the PNZT film is found to be affected by the internal electric field, which could be explained by the barriers between the PNZT films and electrodes. The results indicate that the ferroelectric fatigue and imprint properties of PNZT film could be improved by introducing appropriate top and bottom electrodes.

Graphical Abstract

1 Introduction

Lead zirconate titanate [$Pb(Zr_{1-x}Ti_x)O_3$, PZT] films have been attracting much attention because of their superior ferroelectric properties and potential applications in ferroelectric memory [1]. Ferroelectric fatigue and imprint properties are two of the most important failure mechanisms of these devices. It is found that Nb donor dopant can reduce the oxygen vacancy density and improve the ferroelectric imprint property of PZT films [2, 3]. Single-crystal substrates, such as Nb-doped $SrTiO_3$ (Nb-STO) [4,

✉ Quanliang Zhao
  zql-01@163.com

[1] School of Mechanical and Materials Engineering, North China University of Technology, Beijing 100144, People's Republic of China

[2] School of Materials Science and Engineering, Beijing Institute of Technology, Beijing 100081, People's Republic of China

5], MgO [6] and LaAlO$_3$ [7], are usually used to grow Nb-doped PZT (PNZT) films due to their matched lattice parameters. However, single-crystal substrates are expensive and hard to fabricate large-area films and integrate with conventional silicon-based devices. Recently, some PNZT films have been deposited on the Pt-coated Si substrates [2, 8–10]. It is found that oxygen vacancies that lead to the degeneration of ferroelectric properties are easy to aggregate at the interfaces of metal electrodes. Instead, conductive metal oxide films are good candidates since they have matched lattices with PNZT films. It has been reported that the ferroelectric fatigue property of PNZT films was improved by using LaSrCoO$_3$ and Pb$_{0.8}$La$_{0.1}$Ca$_{0.1}$Ti$_{0.975}$O$_3$ conducting films [11, 12].

Perovskite structural LaNiO$_3$ (LNO) film, a good electrical conductive oxide, has been used as top and bottom electrodes of PZT [13], BaTiO$_3$ [14] and BiFeO$_3$ [15] based films to improve their ferroelectric properties. However, the long-duration ferroelectric fatigue and imprint properties of PNZT film deposited on LNO electrode have not been reported. In this work, Nb$_{0.02}$–Pb(Zr$_{0.6}$Ti$_{0.4}$)O$_3$ (PNZT) films are prepared on LNO/SiO$_2$/Si and Pt/Ti/SiO$_2$/Si substrates with Au top electrodes by a sol–gel route. The effects of the top and bottom electrodes on the long-duration ferroelectric fatigue and imprint properties of PNZT films are investigated.

2 Experimental

In brief, LNO sol (0.3 mol/L) was prepared by a sol–gel route, and nickel acetate and lanthanum nitrate were used as raw materials with a molar ratio of 1:1. PNZT sol (0.5 mol/L) was prepared by using lead acetate, zirconium n-propoxide, tetrabutyl titanate, niobium ethoxide and polyvinylpyrrolidone (PVP, 4.0×10^4 in average molecular weight) with a molar ratio of 1.1:0.6:0.4:0.02:1. LNO thin film was deposited on the SiO$_2$/Si (100) substrate by the spin-coating technique at 4000 rpm for 30 s. Each LNO layer was heated at 120 °C for 3 min and calcined at 400 °C for 20 min to remove the organic components, followed by a rapid annealing at 800 °C for 5 min in the oxygen atmosphere. The thickness and resistivity of the five-layer LNO film were about 300 nm and 1.7 mΩ·cm, respectively. PNZT films were spin-coated on the LNO/SiO$_2$/Si (100) and Pt (111)/Ti/SiO$_2$/Si (100) substrates with a spinning rate of 3000 rpm for 30 s, and then, the wet films were dried at 120 °C for 3 min. Every two-layer PNZT film was calcined at 400 °C for 10 min and annealed at 650 °C for 10 min in the air atmosphere. A PbO capping layer was deposited on the ten-layer PNZT film prior to final annealing at 650 °C for 30 min. The thickness of the as-fabricated PNZT films was about 900 nm. Au top

electrodes (300 μm × 300 μm) were deposited by sputtering with metal mask for measuring electrical properties.

The crystal structures of the PNZT films were analyzed by X-ray diffraction (XRD) with CuKα radiation (Bruker AXS/D8, $\lambda = 0.15405$ nm). The ferroelectric and leakage current properties of the PNZT films were measured by a ferroelectric test system (Radiant, Precision Multiferroic). The dielectric property was measured by the impedance analyzer (Agilent E4990A).

3 Results and discussion

The XRD patterns of the LNO, PNZT/LNO and PNZT/Pt films are shown in Fig. 1. The peak intensity of the LNO film is magnified ten times because it is too weak to be covered by the PNZT film peaks. It is suggested that the LNO and both the PNZT films are in random orientation and have typical perovskite structures.

The ferroelectric hysteresis loops of the PNZT films are shown in Fig. 2a, b. It should be noted that both hysteresis loops are not symmetric, and they shift toward the positive and negative voltage directions for PNZT/LNO and PNZT/Pt films, respectively. The average remnant polarizations and coercive voltages of the PNZT/LNO and PNZT/Pt films with voltage of 30 V are about 17, 19 μC/cm^2, 3.9 and 3.2 V, respectively. Figure 2c, d shows the dielectric and leakage current properties of the PNZT films. The dielectric constants and losses of the PNZT/Pt and PNZT/LNO films are about 982, 599, 0.04 and 0.06 at 1000 Hz, respectively. The ferroelectric fatigue properties of the PNZT films are shown in Fig. 2e, f. It is observed that the fatigue of both films occurs after 10^6 switching cycles and the degeneration of the PNZT/Pt film is faster than that of the PNZT/LNO film. After 10^{10} switching cycles, the average remnant polarizations of the PNZT/Pt and PNZT/LNO films decrease about 60 and 45 %, respectively. This
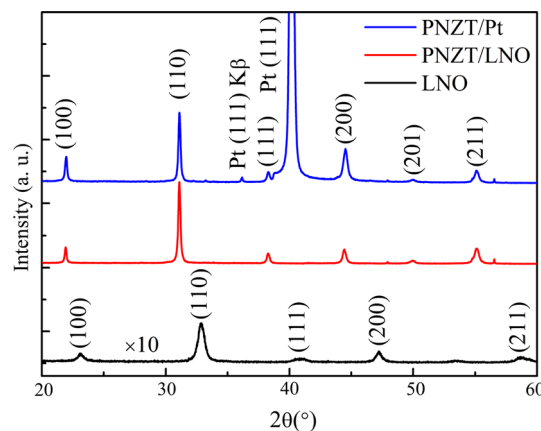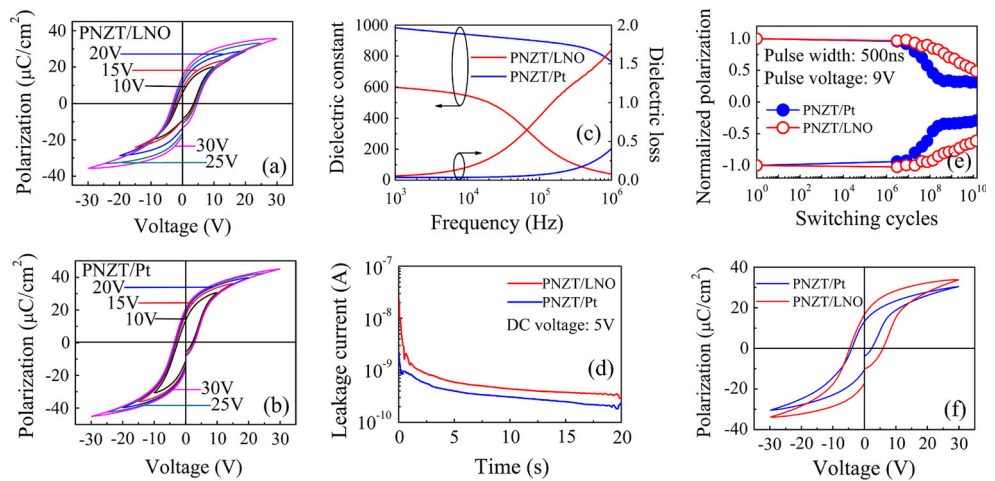

Fig. 1 XRD of the LNO, PNZT/LNO and PNZT/Pt films

Fig. 2 Ferroelectric hysteresis loops of **a** the PNZT/LNO and **b** PNZT/Pt films, **c** the dielectric and **d** leakage current curves, **e** the ferroelectric fatigue curves, **f** the ferroelectric hysteresis loops after 10^{10} switching cycles

indicates that the ferroelectric fatigue property of the PNZT film is improved by using LNO film as a bottom electrode. The reason should be attributed to the oxygen vacancies that are easier to aggregate at the interface of Pt electrode. The aggregated oxygen vacancies play a role of pinning the domain walls and lead to hard polarization switch [12].

The ferroelectric imprint properties of the PNZT/LNO and PNZT/Pt films are shown in Fig. 3. The preset voltage applied on the top electrodes is 30 V. Figure of merit

Fig. 3 **a** Ferroelectric imprint curves of the PNZT/LNO and PNZT/Pt films, **b** the ferroelectric hysteresis loops after 6000-s imprint time

(FOM) is defined as the occurrence of imprint failure when the normalized coercive voltage offset is greater than 1. It is written by the following equation

$$\text{FOM} = [(|V_c(t)| - |-V_c(t)|)/2]/[(|V_{c\,\text{init}}| + |-V_{c\,\text{init}}|)/2],\tag{1}$$

where $V_{c\,\text{init}}$ and $-V_{c\,\text{init}}$ are the positive and negative coercive voltages at the initial state, respectively; $V_c(t)$ and $-V_c(t)$ are the positive and negative coercive voltages at imprint time t. Figure 3a shows that FOM of the PNZT/LNO and PNZT/Pt films decreases to -0.10 and -0.48 after about 6000 s, i.e., the negative voltage offset of the hysteresis loop of PNZT/Pt film is larger than that of the PNZT/LNO film, as shown in Fig. 3b. It should be noted that the initial FOM values are about 0.17 and -0.15 for the PNZT/LNO and PNZT/Pt films, respectively. This means that a negative imprinted polarization state or an internal field toward the top electrode is built in the PNZT/LNO film, while a positive polarization state or an internal field toward the bottom electrode is built in the PNZT/Pt film in the initial state. This is consistent with the asymmetric ferroelectric hysteresis loops with right and left shifts as shown in Fig. 3a, b.

The asymmetric hysteresis loops in the initial state should be attributed to the different work functions of the top and bottom electrodes, as shown in Fig. 4. W_{Au}, W_{Pt} and W_{LNO}, which correspond to the work functions of Au, Pt and LNO, are 5.1, 5.6 and 4.5 eV, respectively [16, 17]. The electron affinity χ of the PNZT film is defined as the difference of vacuum level and conduction level. Due to the substitution of Nb^{5+} ions at the B site (Zr^{4+} or Ti^{4+}) ions, the deposited PNZT films are considered as a n-type semiconductor. When a metal contacts a n-type semiconductor, an internal electric field (E_i) toward metal will be built at the interface. The largest and smallest electric fields locate at the interfaces of the Pt and LNO electrodes, respectively, because of their highest and lowest barriers.
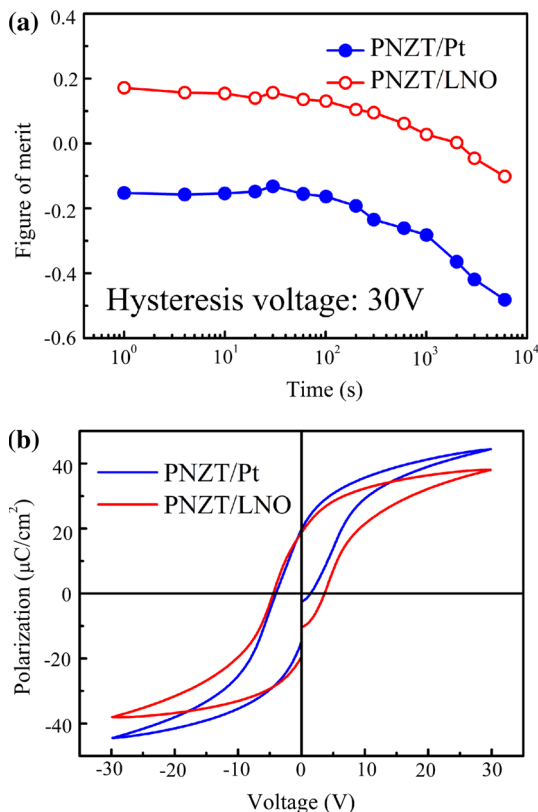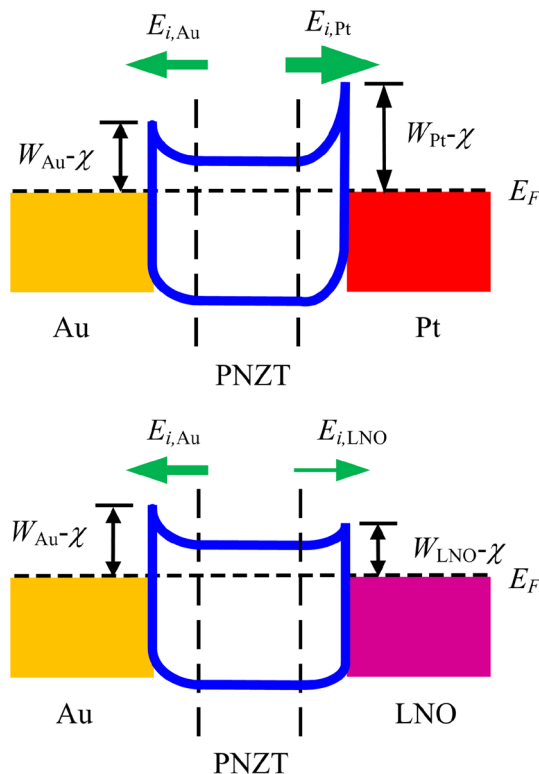
Fig. 4 Energy band diagrams of the PNZT/LNO and PNZT/Pt films with Au top electrodes

Thus, the initial net electric fields are toward the bottom and top electrodes for PNZT/Pt and PNZT/LNO films, respectively. As positive preset voltages applied on the top electrodes, more positive charges are injected and reduce the internal electric fields at the interfaces of the Au electrodes with time increases. The net electric fields toward the bottom electrodes would become greater. On the contrary, it is also suggested that the net electric fields toward the top electrodes would increase when negative preset voltages applied on the top electrodes. This result indicates that the top and bottom electrodes can affect the initial polarization states of the PNZT films. The larger difference of their work functions would result in the greater offset of the initial FOM, which is known as the faster imprint failure.

4 Conclusions

In summary, the PNZT films with well perovskite crystallization have been prepared on the LNO/SiO$_2$/Si and Pt/Ti/SiO$_2$/Si substrates using a sol–gel route. The PNZT/

LNO film shows an improved ferroelectric fatigue property in comparison with the PNZT/Pt film. Ferroelectric imprint has been found to be significantly affected by the initial polarization state, which refers to the work function difference of the top and bottom electrodes. Therefore, ferroelectric fatigue and imprint properties of the PNZT film could be improved by moderating top and bottom electrodes.

References

1. Kim Y, Kim J, Bühlmann S, Hong S, Kim YK, Kim S-H, No K (2008) Phys Status Solidi RRL 2:74–76
2. Kwok KW, Tsang RCW, Chan HLW, Choy CL (2008) J Sol-Gel Sci Technol 47:148–153
3. Sun HJ, Zhang Y, Liu X, Guo S, Liu Y, Chen W (2015) J Sol-Gel Sci Technol 74:378–386
4. Zhu Z-X, Li J-F, Liu Y, Li J (2009) Acta Mater 57:4288–4295
5. Yu Q, Li J-F, Sun W, Zhu F-Y, Liu Y, Chen Y, Wang Z, Li J (2014) Appl Phys Lett 104:012908 (**5 pages**)
6. Puustinen J, Lappalainen J, Lantto V (2008) Thin Solid Films 516:6458–6463
7. Al-Shareef HN, Dimos D, Raymond MV, Schwartz RW, Mueller CH (1997) J Electroceram 1:145–153
8. Yu Q, Li J-F, Sun W (2013) Appl Surf Sci 265:334–338
9. Ferrari P, Ramos-Moore E, Guitar MA, Cabrera AL (2014) Thin Solid Films 556:539–543
10. Fujii T, Hishinuma Y, Mita T, Arakawa T (2009) Solid State Commun 149:1799–1802
11. Dhote AM, Madhukar S, Wei W, Venkatesan T, Ramesh R, Cotell CM (1997) Appl Phys Lett 68:1350–1352
12. Chi QG, Li WL, Wang X, Fei WD, Lei QQ (2011) J Alloys Compd 509:2804–2807
13. Li K, Sama N, Li T, Rémiens D, Du G, Dong X, Wang G (2014) Appl Phys Lett 104:092904 (**5 pages**)
14. Li W, Hao J, Bai W, Zhai J (2013) J Sol-Gel Sci Technol 66:220–224
15. Li H, Zhu J, Zhuang J, Hu Y, Huai M, Yang Q (2015) J Sol-Gel Sci Technol 75:353–359
16. Lee K-W, Kim Y-I, Lee W-J (2002) Ferroelectrics 271:179–185
17. Yang T-H, Harn Y-W, Chiu K-C, Fan C-L, Wu J-M (2012) J Mater Chem 22:17071–17078